Nozzles and Intakes Interacting with the External Flow: Design and Analysis

M.Ferlauto, F.Larocca and L. Zannetti
Dip. Ingegneria Aeronautica e Spaziale,Politecnico di Torino
Corso Duca degli Abruzzi 24,10129 Torino, Italy.
e-mail: ferlauto@athena.polito.it

Abstract

The paper describes a numerical technique for the design and the analysis of the flow in air intakes and nozzles. Interfaces separating internal flows, as in the jet of multiple nozzles, and the external flow are fitted, while shocks or contact discontinuities inside each flow are inherently captured by the numerical scheme. The interaction with the external flow and shape optimization are both concerned in an unified approach which refers to the solution of an inverse problem. The unsteady Euler equations are integrated numerically by using a time-dependent procedure and by adopting an upwind finite volume approximation that belongs to the class of the second order ENO schemes. Several numerical examples are presented.

1 Introduction

The efficiency of propulsion systems is strongly affected by the air intake and the nozzle. Despite their simple geometry, such devices exhibit flow phenomena quite complex over the expected range of operation. The presence of flows having different thermodynamic properties give rise to shear layers strongly interacting with the external flow. This phenomenon is especially relevant to the transonic flight [1], where an even stronger coupling can take place between the above mentioned contact interfaces and shocks. Furthermore, in hypersonic propulsion the high integration of airbreathing engines in the vehicle requires also an accurate prediction of the perfomances of the exhaust system because of its influence on the net thrust. To avoid the use of iterative procedures in the design process, we formulate an inverse problem in which the location of the contact interfaces is not known a priori and their final shape is part of the solution. At the same time other design requirements can be prescribed to optimize the nozzle performance. The numerical method is based on the finite volume approximation of the time-dependent Euler equations according to a second order accurate ENO scheme. Interfaces separating internal flows, as in the jet of multiple nozzles, and the external flow are fitted, while shocks or contact discontinuities inside each flow are inherently captured by the numerical scheme. The design problem of finding the shapes of the solid walls of intakes or nozzles is satisfied the prescibed pressure distributions is solved according to a time-dependent process [2][3][4][7]. The walls are considered impermeable and flexible, an initial shape is assumed and then design pressure and impermeability are imposed as boundary conditions. During the transient the shape changes until a steady state is reached. The same model is used to define the geometry of the fluid interfaces, which are treated as impermeable an flexible walls with the same pressure on their sides. In the next sections the mathematical model and the numerical procedure are illustrated. The technique is then applied to the design of a transonic diffuser and to the study of a dual nozzle configuration interacting with the external flow.

1.1 Governing Equations

The Euler equations for a two-dimensional or axisymmetric unsteady motion of an inviscid compressible fluid, are written in divergence form:

$$\nabla \cdot [\mathbf{V}] = -\frac{\alpha}{y} \cdot \mathbf{N} \qquad (1)$$

with ∇ and $[\mathbf{V}]$ being:

$$\nabla = \frac{\partial}{\partial t}\mathbf{k} + \frac{\partial}{\partial x}\mathbf{i} + \frac{\partial}{\partial y}\mathbf{j} \qquad [\mathbf{V}] = \{\mathbf{U}\}\mathbf{k} + \{\mathbf{F}\}\mathbf{i} + \{\mathbf{G}\}\mathbf{j}$$

where $\alpha = 0$ for 2-D flow and $\alpha = 1$ for axisymmetric flow, $\mathbf{i}$, $\mathbf{j}$, $\mathbf{k}$ are the unit vectors of a Cartesian frame of reference of the 3D space-time (x, y, t), and

$$\mathbf{U} = \begin{Bmatrix} \rho \\ \rho u \\ \rho v \\ e \end{Bmatrix} \qquad \mathbf{F} = \begin{Bmatrix} \rho u \\ p + \rho u^2 \\ \rho uv \\ (e+p)u \end{Bmatrix}$$

$$\mathbf{G} = \begin{Bmatrix} \rho v \\ \rho uv \\ p + \rho v^2 \\ (e+p)v \end{Bmatrix} \qquad \mathbf{N} = \begin{Bmatrix} \rho v \\ \rho uv \\ \rho v^2 \\ (e+p)v \end{Bmatrix}$$

ρ, p, e, denote density, pressure and internal energy per unit volume, respectively, while u, v are the Cartesian components of the flow velocity. All the flow properties are normalized with respect to suitable reference values.
According to the Gauss formula, the integral of eq. (1) in a given volume D of the space-time can be written as:

$$\int_{\partial D} [\mathbf{V}] \cdot \mathbf{n} d\sigma = -\alpha \int_D \frac{\mathbf{N}}{y} d\tau \qquad (2)$$

with ∂D being the boundary of the volume D and $\mathbf{n}$ the outward normal. Eq. (2) is approximated by a finite volume technique by discretizing the (x, y) plane by means of four sided cells whose shape depends on time. The integration in time is carried on according to a Godunov type two-step scheme [9]. At the *predictor* step, a standard first order FDS is used: the primitive variables (ρ, p, e, u, v) are assumed at a constant average value inside each cell. The fluxes $\mathbf{F}$, $\mathbf{G}$ are evaluated by solving the Riemann's problems pertinent to the discontinuities that take place at the cells interfaces. To this purpose, we adopted the approximate Riemann solver suggested in [6]. At the *corrector* level, the second order of accuracy is achieved by assuming a linear, instead of constant, behaviour of the primitive variables inside the cells, according to the ENO concept ([8], [9]). The resulting scheme is second order accurate in both time and space.

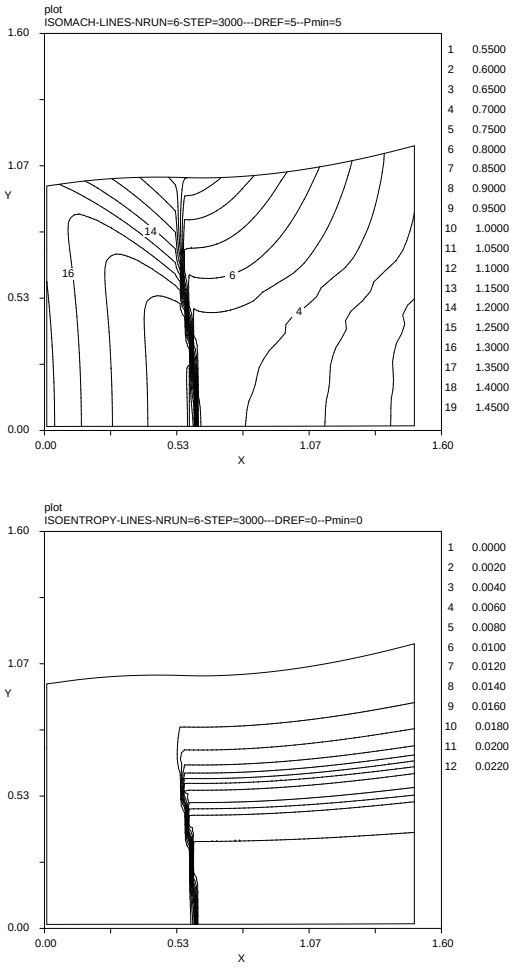

Figure 1: Transonic diffuser: *a*) isoMach *b*) isoentropy

1.2 The boundary conditions

The computational domain is bounded by artificial (i.e. far field boundaries) and physical contours (i.e. impermeables walls), that can be solid, as in the direct problem, flexible, as in the inverse problem, or partly solid and partly flexible. The theory of characteristics states the number of conditions to be imposed at each boundary of the computational domain. For examples, one boundary condition is nedeed at impermeable boundaries; it is prompted by the physics of the problem: at a solid wall the vanishing of the velocity component normal to the wall is imposed, while at a flexible wall, according to the inverse problem formulation, the design pressure is prescribed. The computation at the boundaries is carried out by solving an *half Riemann problem*, as described in [10]. At a deformable wall, once the flow properties are computed, the geometry is updated by enforcing the condition of impermeability: each point of the wall has to move with a normal velocity equal to the normal component of the flow velocity, as described with details in [2]. The same method here described to solve inverse problems can be used to determine the shape of plumes and interfaces. For instance, the streamtube confining a jet in air at rest can be seen as the wall of a duct along which costant pressure is prescribed. Moreover, in flow regions, such as after-bodies or dual nozzles in by-pass turbofans, contact discontinuities are generated by different stagnation conditions and thermodynamic properties of the incoming flows. Such discontinuities are interfaces that can be computed explicitly according to the present method: they are considered as impermeable and deformable walls across which pressure and normal component of the flow velocity are imposed to be continuous.

2 Numerical results

2.1 Transonic diffuser

The first example deals with the design of a transonic diffuser. The design pressure along the unknown upper wall is prescribed according to the law:

$$p_d = p_{in} + (p_e - p_{in})\,(x/l) \qquad (3)$$

with $p_{in} = 0.4$, $p_e = 0.75$, $P^0 = 1$. The lower wall is assumed solid. The inlet flow is assumed supersonic, while a subsonic condition is imposed at the exit. Figs 1 *a)* and *b)* show the final geometry with the iso-mach and isoentropy contours respectively. The pictures exhibit the transition from supersonic to subsonic regime through a shock wave in the flow core but shockless at wall, as it should be expected, since the design pressure is prescribed as a continuous function along the wall.

2.2 Dual nozzle configuration with external flow

In this example we show the computation of a dual nozzle and jet. The wall geometry of the external nozzle and and the shapes of the interfaces confining the inner and outer flows are determined according to the inverse procedure. The computational domain is divided in two regions: the inner region which represent an 'internal flow' bounded by the centerline, the inner nozzle contour and the contact discontinuity; the outer region is confined by the external nozzle walls, the contact discontinuity and a free pressure boundary. The inner nozzle has an half-angle equal to 5^o, while the external one has 10^o divergence angle. The inlet flow is supersonic for both nozzles, but with different total conditions. At the inner nozzle we prescribe total pressure $p^0 = 1.0$, total temprerature $T^0 = 1.0$ and Mach number $M = 2.0$; at the inlet of the external nozzle we impose $p^0 = 0.9$, $T^0 = 1.0$ and $M = 1.8$. The external pressure is $p_e = 0.07$. Moreover, along the upper wall of the secondary nozzle, a design pressure distribution is set according to

$$p_d = (p_{in} - p_e)\sin(\pi\, x/1.5) \qquad 0 < x < 1.5$$
$$p_d = p_e \qquad 1.5 < x < 2.5$$

where $p_{in} = 0.1566$ and $p_e = 0.07$. The above pressure distribution allows the secondary nozzle to be fully expanded with a nearly uniform axial flow at the exit section. The resulting flow configuration and the geometry of the swecondary nozzle are shown in fig. 2. The isoMach contours, plotted in fig. 2 *a*, reveal the presence of an oblique shock wave,

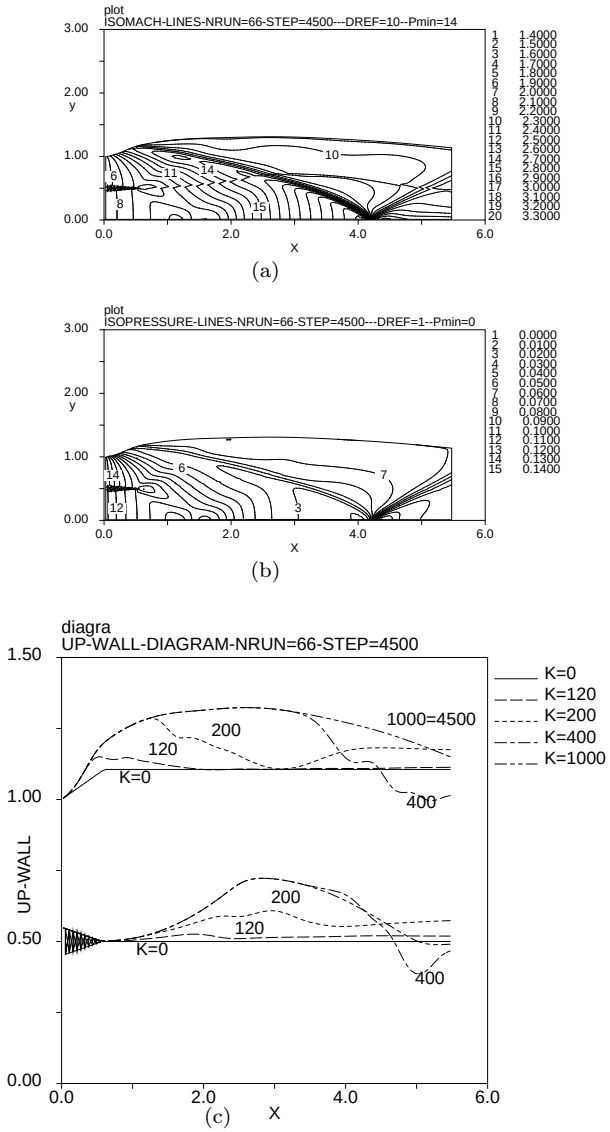

Figure 2: Dual nozzle: *a*) isoMach, *b*) isopressure *c*) time evolution

due to the change of wall curvature.In fig. 2 *b* isopressure contours show a continuous behavior across the interface. The evolution in time of the jet contour and the interface are given in fig. 2 *c*. The starting configuration is characterized by straight lines for the jet boundary and interface ($K = 0$). The final steady configuration is obtained after $K = 1000$ time steps.

2.3 Flow past a turbofan-nacelle-like configuration

The final example refers to the flow past a turbofan-nacelle-like configuration. The flow is assumed axisymmetric and the computational domain is divided in three parts: I) the region pertinent to the inner nozzle, which is bounded by the centerline, the

inner nozzle contour and the contact discontinuity separating the hot flow and the cold flow; II) the region pertinent to the outer nozzle, which is bounded by the above mentioned contact discontinuity and a second one, separating the cold flow from the external flow: III) the external flow field. The present numerical example refers only to the afterbody region, comprehensive of the nozzles and multiple-jet flow. As test-case and for sake of simplicity, we imposed in all the three regions identical inlet conditions: $P^0 = 1.$, $T^0 = 1.$ and $M = 0.5$. The external pressure is $p_e = 0.843$. In the complete model, which is work in progress, the effective inlet conditions are given by the engine, which is modelled as a black box that receives the flow through the intake and return back flows with different total pressure and total enthalpy to the nozzles. The isopressure lines and the computed shapes of the plumes and inner interfaces are plotted in fig3, as well as the visualization of the velocity field.

3 Conclusions

A numerical technique has been proposed to combine optimized design of air intake and nozzles, taking into account the interaction with the external flow inherently. The procedure lead to an inverse problem, solved in a time-dependent fashion. Several numerical examples have been also presented to explain the most important aspects of the methodology. This work is the kernel of a model for the entire flow past a turbofan nacelle, in the inlet, nozzles and multiple-jets flow, where the engine will be modeled as a black box that receives the flow through the intake and return back flows with different total pressure and total enthalpy to the nozzles.

References

[1] D.J. Dusa, IX ISABE, 1989, Athens, Greece.

[2] L. Zannetti, AIAA J., Jul. 1980, pp. 754-758

[3] L. Zannetti, M. Pandolfi, NASA CR 3836, 1984

[4] L. Zannetti, T. T. Ayele, AIAA 25th Aer. Sp. Scien. Meet., AIAA-87-0007.

[5] S. Osher, F. Solomon, Mathematics of Computation, vol. 38, 1982.

[6] M. Pandolfi, AIAA J. n. 5, vol. 22, 1984.

[7] F. Larocca, L. Zannetti, 11th Int. Symp. on Air Breathing Engines, 1993, Tokyo, Japan

[8] Harten et al., J. Comput. Phys. 71 (1987),231.

[9] A. Di Mascio, B. Favini, Meccanica, Vol. 26, 1991.

[10] F. Larocca, L. Zannetti AIAA Paper 95-0648, 1995.

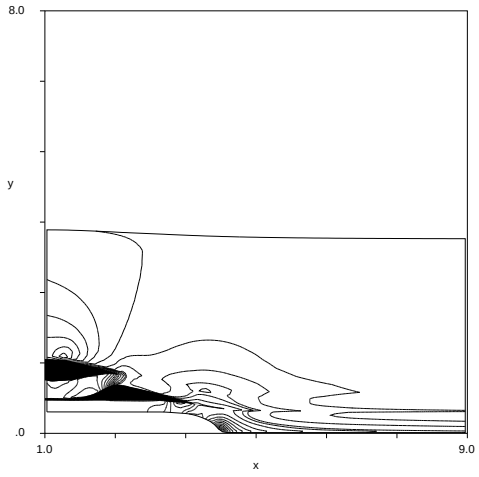

(a)

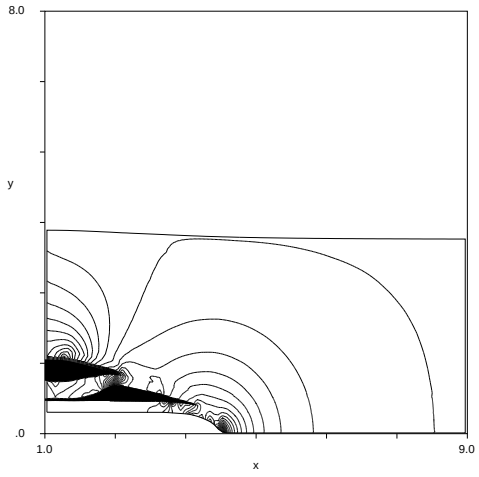

(b)

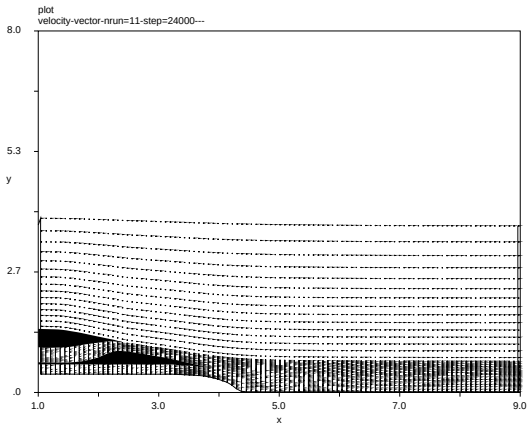

(c)

Figure 3: Flow past a turbofan-nacelle-like configuration: a) isoMach, b) Isopressure, c) streamlines.